Progress in Nuclear Energy 111 (2019) 74–84

Contents lists available at ScienceDirect

Progress in Nuclear Energy

journal homepage: www.elsevier.com/locate/pnucene

Research of coupled wall conduction effects on forced and natural circulation of LBE in CLEAR-S

Muhammad Younas Ali[a,b], Guowei Wu[a,*], Shuyong Liu[a], Ming Jin[a], Jin Wang[a]

[a] Key Laboratory of Neutronics and Radiation Safety, Institute of Nuclear Energy Safety Technology, Chinese Academy of Sciences, Hefei, Anhui, 230031, China
[b] University of Science and Technology of China, Hefei, Anhui 230027, China

ARTICLE INFO

Keywords:
LBE
CLEAR-S
Wall conduction
Forced circulation
Natural circulation
FLUENT

ABSTRACT

The lead based reactor concept is considered to be the most promising reactor option for the Accelerator Driven Subcritical (ADS) system. Lead based reactor engineering validation facility CLEAR-S is a large scale integrated non-nuclear pool type facility which has been built to provide a unique experimental platform for full-scale prototype components test of lead based reactors. In this article, three-dimensional steady state analysis of flow in the hot and cold pools of CLEAR-S was carried out by using computational fluid dynamics (CFD) code FLUENT during forced and natural circulation conditions. The results showed that the simulation had a good agreement with the design parameters of CLEAR-S and the temperature profile was uniform in the whole domain of the hot and cold pools without considering any conduction through the coupled walls. The temperature distribution in the hot and cold pools became non-uniform with the coupled wall conduction and thermal stratification was observed in the cold and hot pools near the bottom wall of the hot pool. This non-uniform distribution of temperature could cause thermal stresses on equipment, which is dangerous for the integrity of the system. During natural circulation conditions, the coupled wall conduction enhanced the natural circulation and kept the hot pool at a relatively low temperature because the cold pool cooled the hot pool through heat transfer between the walls of the hot and cold pools. Therefore, wall conduction has some advantages and disadvantages as it enhances the natural circulation on one hand but disturbs temperature uniformity on the other hand.

1. Introduction

The lead based reactor concept (lead cooled or lead bismuth cooled reactor), which is one of the Generation-IV nuclear energy systems is considered to be the most promising reactor option for the Accelerator Driven Subcritical systems (ADS) (Wu, 2016a). Chinese Academy of Sciences (CAS) launched an engineering project to develop Accelerator Driven System (ADS) for nuclear waste transmutation in 2011 (Wu et al., 2015, 2016a). China Lead based Research Reactor (CLEAR-I) proposed by Institute of Nuclear Energy Safety Technology (INEST), CAS was selected as the reference reactor in this ADS project (Wu et al., 2011, 2015). INEST has conducted a lot of research on lead based reactors including reactor concept, coolant technology, key components, materials and fuel, operation and control etc. (Huang et al., 2007, 2013; Huang, 2017; Wu and FDS Team, 2006, 2009; Wu, 2007, 2008, 2018). Lead based reactor engineering validation facility CLEAR-S is a large scale integrated non-nuclear pool type facility which has been built to provide a unique experimental platform for full-scale prototype components test of lead based reactor under steady state and transient conditions (Wu et al., 2016b; Wu, 2016b). Loss of coolant flow accident is highly probable in lead based reactor. This type of accident occurs due to sudden shutdown of primary coolant pump caused by power failure, pump malfunctioning or flow blockage etc. Hence, coolant mass flow rate suddenly decreases and the system shifts itself from forced circulation (FC) to the natural circulation (NC) during loss of coolant flow accident. In natural circulation condition, there is the possibility of non-uniformity of temperature or the occurrence of thermal stratification in the reactor pools. Thermal stratification is hazardous for the integrity of reactor components because it can create thermal shocks and also increases the thermal stress.

There were some experimental and computational studies carried out in this field. In 1985, M. Miksch et al. studied the effects of thermal stratification on horizontal feed water pipes of light water reactor (LWR) during loading conditions. It was illustrated from their results that a particular type of cracks was formed on the horizontal feed water piping of steam generator and reactor pressure vessel (RPV) due to the thermal shocks generated by stratification (Miksch et al., 1985). S. Moriya et al. used the simplified model of hot plenum of pool type

* Corresponding author.
E-mail address: guowei.wu@fds.org.cn (G. Wu).

https://doi.org/10.1016/j.pnucene.2018.10.009
Received 15 March 2018; Received in revised form 14 September 2018; Accepted 19 October 2018
Available online 08 November 2018

List of abbreviations

ADS	Accelerator Driven System
CLEAR-S	Lead based reactor engineering validation facility
CFD	Computational Fluid Dynamics
LBE	Lead Bismuth Eutectic
CAS	Chinese Academy of Sciences
CLEAR-I	China Lead based Research Reactor
INEST	Institute of Nuclear Energy Safety Technology
RPV	Reactor Pressure Vessel
LWR	Light Water Reactor
LMFBR	Liquid Metal Fast Breeder Reactor
HDR	Superheated steam reactor
X-ADS	eXperimental Accelerator Driven System
HX	Heat Exchanger
DHR	Decay Heat Removal
CIRCE HLM	CIRColazione Eutettico Heavy Liquid Metal
FC	Force Circulation
NC	Natural Circulation
UDF	User Define Function
CP	Cold Pool
HP	Hot Pool

liquid metal fast breeder reactor (LMFBR) to examine the effects of Reynolds and Richardson number on thermal stratification (Moriya et al., 1987). A. Talja and E. Hansjosten made a comparison between measured and analytical values of wall temperature difference on the basis of superheated steam reactor (HDR) thermal stratification experiment (Talja and Hansjosten, 1990). J. H. Kim et al. explained that thermal stratification, striping and cycling phenomena were the significant safety concern for the nuclear industry (Kim et al., 1993). In 2016, Byeongnam Jo et al. experimentally investigated the thermal stratification by using suppression pool of Fukushima Daiichi nuclear power plant in sub atmospheric pressure conditions using 1/20 scale torus shaped setup (Jo et al., 2016). Dogan Erdemir et al. enhanced thermal stratification by placing obstacles inside the vertical mantled hot water tanks in order to store thermal energy (Erdemir and Altuntop, 2016). SEOK-KICHOI et al. and M. Shibahara et al. used commercial code, CFX-13 and FLUENT 12.1 to perform the thermal stratification analysis of simplified model of Japanese prototype fast breeder reactor Monju reactor (CHOI-SEOK-KI, 2013; Shibahara et al., 2013). V. Anissimov et al. performed the steady state analysis of experimental accelerator driven system (X-ADS) downcomer channel by using CFX-4.4 in order to study the position and intensity of thermal stratification (Anissimov and Alemberti, 2006). Mariano Tarntino et al. concluded that thermal stratification phenomena had been observed between the outlet of heat exchanger (HX) and decay heat removal system (DHR) based on the first experimental series in CIRColazione Eutettico heavy liquid metal (CIRCE HLM) large pool. In addition, temperature stratification moved downwards as the flow shifted from forced circulation to natural circulation (Tarantino et al., 2015). However, there was no specific research literature available which accounted the effects of coupled wall conduction in pool type reactors. In pool type reactors,

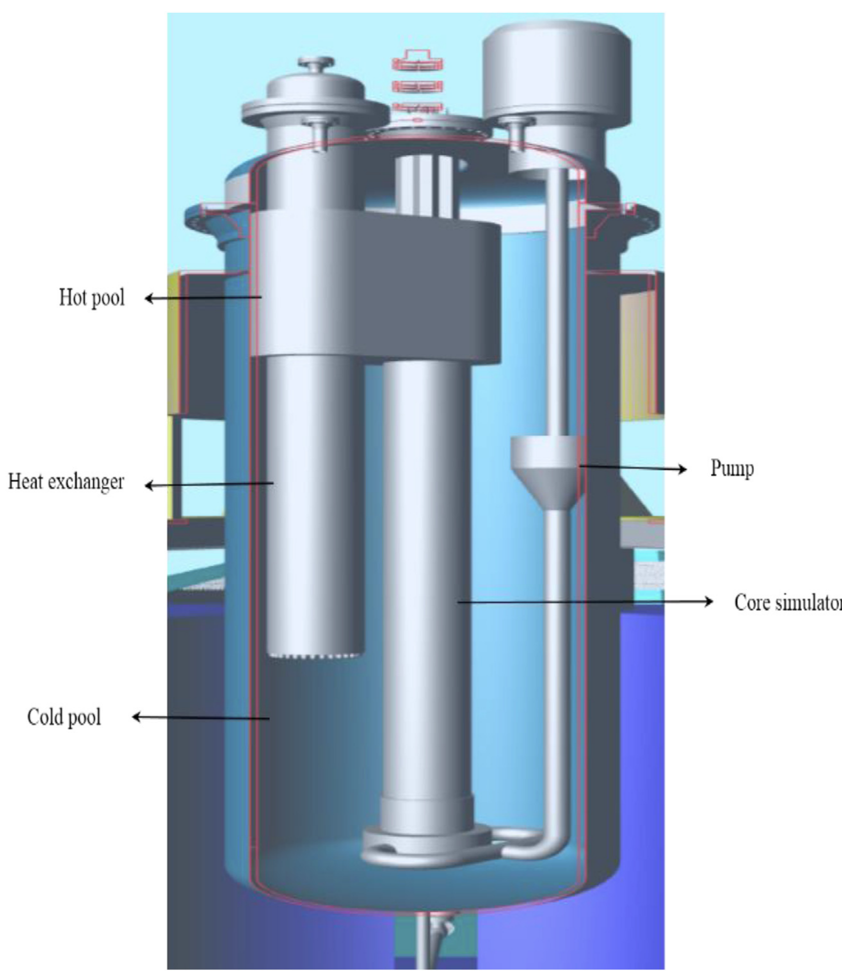

Fig. 1. The schematics of CLEAR-S.

different components were located in a pool. Walls of components were common between pool and each component. So, heat transfer through walls had a definite role in defining the temperature profile of reactor pools during forced and natural circulations and this is the main motivation of research on the above mentioned topic.

In this research, the computational fluid dynamics (CFD) analysis of CLEAR-S was performed by using FLUENT15.0 in order to study the effects of wall conduction on temperature profile of LBE in different components of CLEAR-S. The steady state flow of CLEAR-S was simulated under forced and natural circulations conditions. In the first case, the flow was simulated under forced circulation without any heat transfer through the coupled walls. The forced flow with the conduction through coupled walls was simulated as the second case in order to understand the effects of coupled wall conduction during forced circulation conditions. This case was used to validate the model by comparing simulation results with designed parameters of CLEAR-S. In Case III and Case IV, natural circulation was simulated without and with coupled walls conduction, respectively in order to understand the effects of heat transfer through coupled walls in natural circulation.

2. Numerical models and methods

2.1. CLEAR-S introduction

Fig. 1 shows the schematics of CLEAR-S. It consists of a large LBE pool called cold pool, and all other components like pump, core simulator, HX, Decay heat removal (DHR) and hot pool are located in the cold pool. The pump takes suction of lead-bismuth eutectic (LBE) at 573 K from the cold pool and drives it towards 2.5 MW_{th} non-nuclear core simulator which contains electric fuel pin simulator. The outlet of core simulator is in the hot pool which delivers LBE at 653 K to the hot pool. The hot pool is double wall made up of steel. There is a 100 mm gap filled with air between the double layer walls of the hot pool. HX takes suction from the hot pool and delivers the LBE back to the cold pool at 573 K. In this way the process continues in close cycle and the pump maintains a constant flow of around 220 kg/s. When the pump suddenly shuts down, LBE starts natural circulation. The mass flow rate decreases at that moment and the core simulator power reduces to the 7% of the rated value. The DHR starts cooling and the HX stops its cooling function. Table 1 shows the important design parameters of CLEAR-S.

2.2. Computational model

CFD commercial code ANSYS FLUENT (ANSYS FLUENT 15.0, 2013) was used to perform all the simulations presented in this study. Computational domain of this project was the whole primary coolant flow of CLEAR-S which included the pump, core simulator, hot pool, HX, cold pool and DHR. Energy source used for heating in core simulator was considered as constant while the cooling sources in HX and DHR were defined by User Defined Function (UDF). UDF was a program written in C++ in which the cooling source was defined as a function of temperature difference between average LBE temperature and boiling point of cooling liquid (water). HX UDF was interpreted in FLUENT and hooked in HX zone during forced circulation. During natural circulation, DHR UDF was interpreted and hooked in DHR zone. UDF was added to match the actual condition of HX because heat transfer between the fluids varies with the temperature gradient between primary and secondary fluids. The conduction model was used to set the wall conduction. The hot pool wall was defined as three layered shell of 10 mm thickness for each layer as shown in Fig. 2(b). Layers 1 and 3 were made up of steel and layer 2 was filled with air. Walls of core simulator, HX and DHR were single layered made up of steel. A constant momentum source was used in the pump region in order to simulate the mass flow of forced circulation in CLEAR-S.

Physical properties of LBE had been set as a function of temperature in this simulation in order to study thermal stratification, because this phenomenon occurs due to the variation of density with temperature. LBE was defined in FLUENT according to the data of NEA hand book of LBE (Nuclear Energy Agency, 2015). Important physical parameters used to define LBE are as follows.

$$\rho = 11065.0 - 1.3236T$$

$$C_p = 159 - 2.72 \times 10^{-2}T + 7.12 \times 10^{-6}T^2$$

$$\lambda = 3.61 + 1.517 \times 10^{-2}T - 1.741 \times 10^{-6}T^2$$

$$\eta = 0.027 - 8.93 \times 10^{-5}T + 1.629 \times 10^{-7}T^2 - 1.352 \times 10^{-10}T^3 + 4.25 \times 10^{-14}T^4$$

Where ρ is density in kg/m^3, C_p is specific heat in J/(kg·K), λ is thermal conductivity in W/(m·k), η is viscosity in kg/(m·s), T is temperature in K (Nuclear Energy Agency, 2015; X. Liu and N. Scarpelli, 2015).

In this study, ANSYS ICEM was used for generating hexahedral unstructured mesh. Boundary layer grids were meshed in fluid domains adjacent to the structural wall. Different views of refined grid on different components of CLEAR-S are shown in Fig. 2(b). Mesh convergence study was carried out by varying the grid in axial and radial direction. When the elements were 34.85 million in total, results became grid independent. The total block numbers were more than 5 million. The mean quality of the mesh was 0.92 and the face area and volume were positive. The computational domain of this simulation was from the bottom of the cold pool up to the LBE level, including DHR, the hot pool, HX and the core simulator. Fig. 2 (a) provides the detail idea about computational domain used in this study.

2.3. Numerical methods

Standard $k - \varepsilon$ model with standard wall function was used for the calculations presented in this study because it was used for LBE cooled fast reactor applications (Cheng and Tak, 2006) and is found to be reasonably accurate and efficient (ANSYS FLUENT 14.0, 2011).

In order to simulate FC and NC with wall conduction, appropriate wall thicknesses and materials were set for the walls of Core simulator, HX, DHR and pump to consider proper thermal resistance across the walls. Shell conduction approach was selected for walls of the hot pool, because it was double wall pool with a gap of 10 mm (filled with air) between both walls. For FC and NC without wall conduction, all the walls of CLEAR-S were set to be adiabatic by setting heat flux to zero in wall boundary conditions.

Porous structures like fuel pin simulator and cooling tubes were present in core simulator, HX and DHR which would provide additional pressure drop in these zones. During forced circulation, porous media model was used in core simulator and HX in order to simulate the flow resistance provided by porous structure in these components. During natural circulation, pump impeller also became porous structure because it hinders the flow of LBE. Thus during natural circulation, porous media model was used in core simulator, HX, DHR and pump zones in order to simulate the flow resistance provided by porous structure in these components. Porous media was modeled by the addition of momentum source term in the standard fluid flow equation. In this

Table 1
CLEAR-S design parameters.

Items	Design parameters
Mass flow rate (During FC)	220 kg/s
Mass flow rate through DHR (During NC)	13 kg/s
Pressure drop in core simulator (During FC)	0.8 bar
Pressure drop in HX (During FC)	Less than 0.01 bar
Cold pool temperature (During FC)	573 K
Hot pool temperature (During FC)	653 K
ΔT between the cold and hot pools (During FC)	80 K

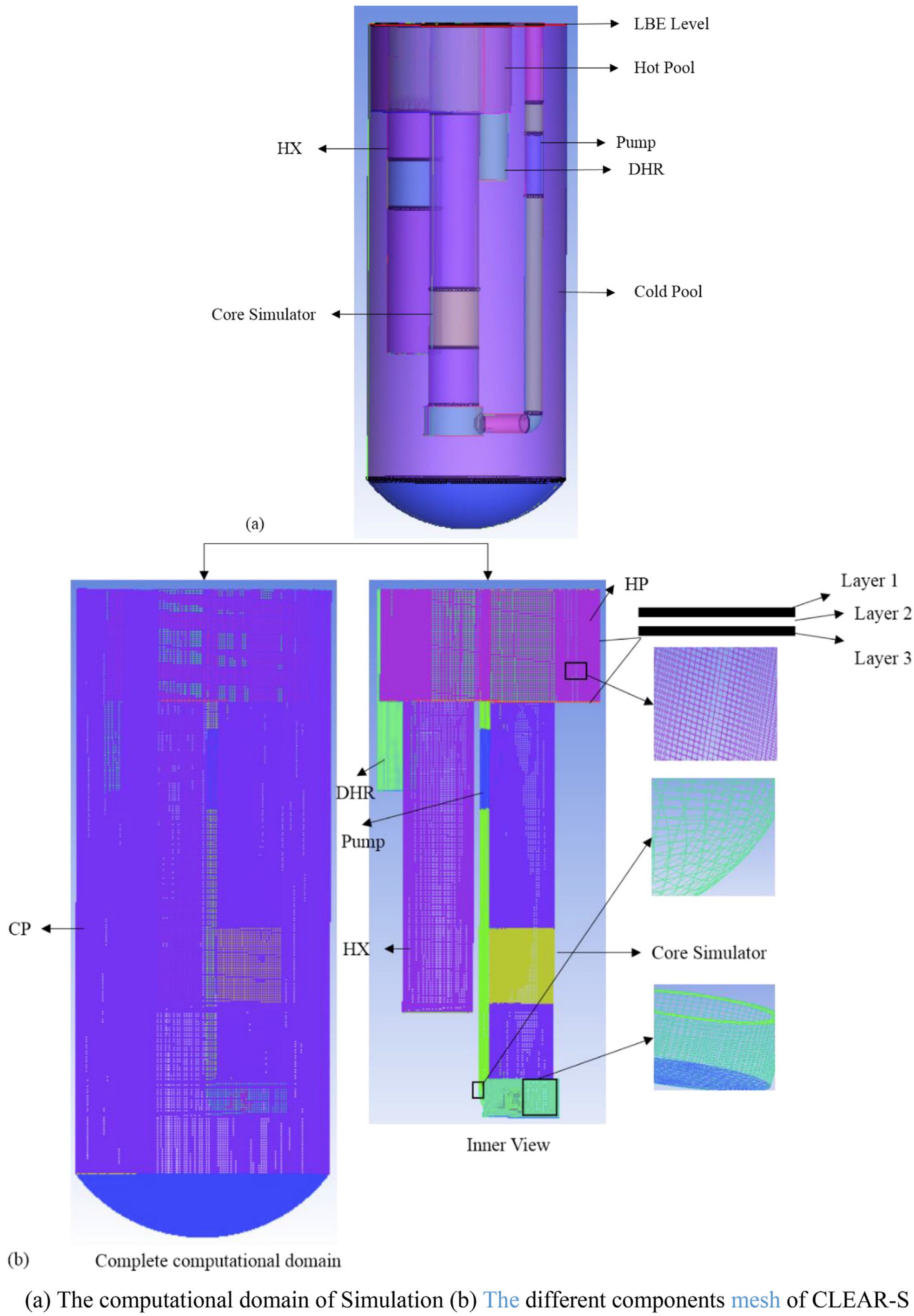

Fig. 2. The numerical model of CLEAR-S.

calculation, pressure drop in core simulator, HX and DHR of CLEAR-S was set equal to the thermal hydraulic design parameters of CLEAR-S by using porous media model.

3. Comparison of simulated results with design parameters

In order to check the accuracy of the simulation, forced flow with coupled wall conduction was simulated and the values of mass flow rate, temperature and pressure drop in core simulator and HX were calculated. These calculated values were compared with the design values of CLEAR-S. Comparison is tabulated in Table 2.

4. Results and discussion

In this section, CFD analysis of CLEAR-S was carried out by using FLUENT in order to study the effects of wall conduction on the temperature profile of LBE in different components of CLEAR-S. The simulation conditions for each case are listed in Table 3.

4.1. Wall conduction effects on FC

4.1.1. Case-I: FC without considering wall conduction

Fig. 3 shows the temperature contours of LBE in CLEAR-S, when the pump worked under normal conditions and provided a constant mass flow of 221.2 kg/s which was approximately equal to the design value of CLEAR-S. In this calculation, adiabatic boundary conditions were set for coupled walls, which meant that there was no heat transfer between pools through the walls. The only way of heat transfer among the pools was the flow of coolant between the pools. The temperature was high in the core simulator due to the presence of core electric fuel pin simulator, which heated the LBE from the cold pool. The temperature dropped in the HX due to the heat transfer between primary and secondary coolants. Therefore, the system attained a constant temperature of about 571.4 K and 652 K in the cold and hot pools, respectively which was almost equal to the designed parameters of CLEAR-S.

Fig. 4 shows the velocity vectors of LBE in CLEAR-S, when the pump worked under normal conditions. The maximum velocity of coolant (about 1.4 m/s) was observed at the corner of the outlet pipe of pump, which was about 10 times higher than the velocity of coolant in other components. The flow from HX to pump passed through the bottom of the cold pool, which means there was no stagnant zone in the system. The velocity vectors in Fig. 4 show that the flow direction was consistent with that of CLEAR-S.

4.1.2. Case-II: FC with wall conduction

Fig. 5 shows the temperature contours of LBE in CLEAR-S, when the pump worked properly and provided a constant mass flow of coolant, which was equal to the designed value of CLEAR-S. In this calculation, wall conduction was set for the coupled walls, which means that there was a heat transfer between the pools and other components of CLEAR-S through the walls. The wall thickness of 10 mm was set for core simulator and HX and a thickness of 7 mm was considered for DHR. These walls were made up of steel. The hot pool was a shell consisting of three layers of 10 mm thickness. Layer 1 and layer 3 were made up of steel while layer 2 was gap filled with air according to the designed parameters of CLEAR-S. Temperature in the core simulator was high due to the presence of electric fuel pin simulator, which heated the LBE. This hot LBE was accumulated in the hot pool and the average hot pool temperature was 648.9 K, which was 3.1 K less than that without considering the wall conduction. The temperature in the HX was dropped due to the heat transfer between the primary and secondary coolants. The average cold pool temperature was 573.6 K, which was about 2.2 K higher than the average cold pool temperature calculated without wall conduction. Therefore, the decrease of temperature in the hot pool and the increase in the temperature of the cold pool were the result of heat transfer from core simulator, hot pool and HX to the cold pool through the coupled walls. The total heat transfer through hot pool, core simulator shell and HX shell was 1.75 kW, 65.01 kW and 27.26 kW, respectively. The total heat transfer through the coupled walls of all components of CLEAR-S during forced circulation was 94.02 kW which was 3.7% of total heat generated by the core simulator. The temperature difference between the cold and hot pools was 75.3 K, which means that the temperature difference decreased from the designed value by 4.7 K. It was clear from Fig. 5 that the temperature profile was not uniform in the hot and cold pools. The temperature stratification near the wall between the hot and cold pools could cause thermal stress and was hazardous for the integrity of the system.

Fig. 6 shows the velocity vectors of LBE in CLEAR-S, when the pump provided a constant mass flow of coolant, which was equal to the designed value of CLEAR-S. Flow from HX to the pump passed through the bottom of the cold pool, which means that there was no stagnant zone in the system. The velocity vectors in Fig. 6 indicate that the flow

Table 3
The simulation conditions for different cases.

Case No.	Name	Simulation conditions
I	FC without considering wall conduction	Coupled walls: adiabatic Pump: working Core simulator: working full power HX: working DHR: Stops
II	FC with wall conduction	Coupled walls: conducting Pump: working Core simulator: working full power HX: working DHR: Stops
III	NC without considering wall conduction	Coupled walls: adiabatic Pump: stops Core simulator: working 7% power HX: Stops DHR: working
IV	NC with wall conduction	Coupled walls: conducting Pump: stops Core simulator: working 7% power HX: Stops DHR: working

Table 2
The comparison between simulation and designed parameters during FC.

Items	Simulation results	Design parameters	Percentage error
Mass flow rate	221.20 kg/s	220.0 kg/s	0.54
Mass flow rate through DHR	13.25 kg/s	13.0 kg/s	1.90
Pressure drop in core simulator	0.79 bar	0.8 bar	1.20
Pressure drop in HX	0.01 bar	Less than 0.01 bar	–
Cold Pool Temperature	573.60 K	573.0 K	0.10
Hot Pool Temperature	648.90 K	653.0 K	0.62

The comparison showed that the error between the simulation results and the design parameters was within 2%.

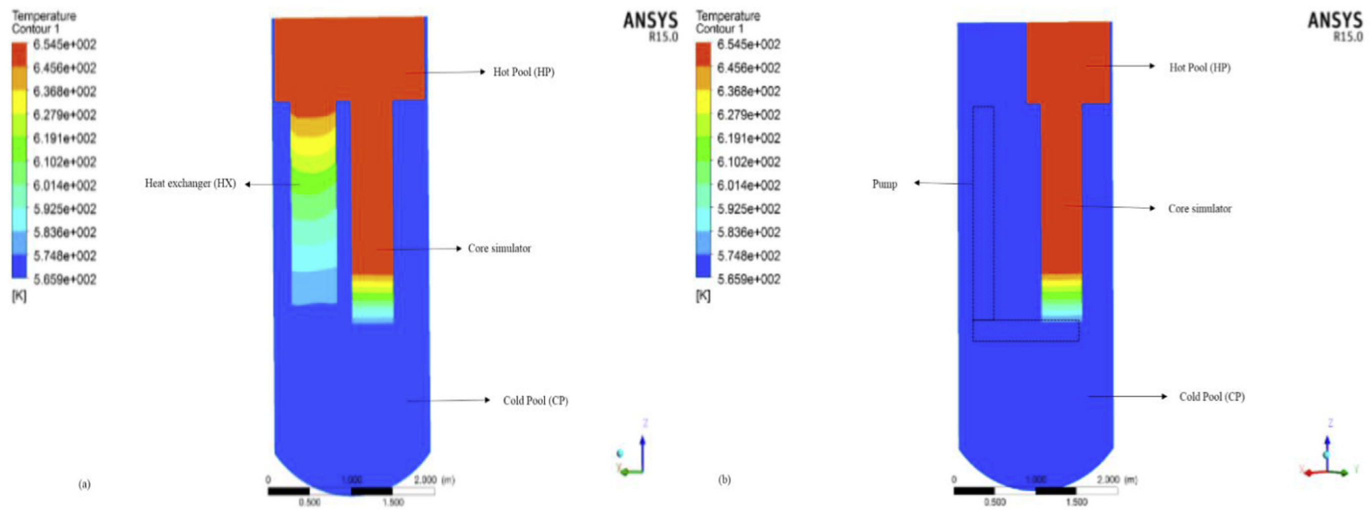

(a) The plane consist of CP, HP, Core simulator & HX (b) The plane consist of CP, HP, Core simulator & Pump

Fig. 3. The temperature contours of LBE under forced circulation conditions without wall conduction in CLEAR-S.

direction was in accordance with that of CLEAR-S.

Fig. 7 shows the axial temperature distribution with and without wall conduction in the cold and hot pools of CLEAR-S, respectively. The average, maximum and minimum temperatures of LBE in the cold and hot pools were tabulated in Table 4 for both cases. It was clear from the graph that the temperature was almost uniform in the hot and cold pools during case I, when the wall conduction was ignored. Difference between T_{max} and T_{min} was only 5.2 K and 4.5 K in the cold and hot pools, respectively for case I, while this difference became 24.5 K and 23.3 K in the cold and hot pools, respectively for case II. This non-uniformity of temperature could cause thermal stresses on components, which was hazardous for the integrity of system. Therefore, these thermal stresses should be included during the stress analysis of the structure.

4.2. *Wall conduction effects on natural circulation*

4.2.1. *Case-III: NC without considering wall conduction*

Fig. 8 shows the temperature contours of LBE, when the pump was shut down and the flow shifted from forced circulation to natural circulation. In this scenario, CLEAR-S shifted from normal operation to DHR mode. In DHR mode, core simulator power reduced to 7% (175 kW) of its rated power. The primary HX was shut down and the required cooling was provided by DHR, which is placed in the cold pool. The mass flow rate decreased up to 6.8 kg/s. The hot pool temperature had a big increase and its average value reached up to 738.6 K, which was about 87 K higher than the hot pool temperature during normal operation. The cold pool temperature decreased and the minimum temperature reached up to 530.6 K. The temperature difference between the fluids of HX and the cold pool that were mixed at the outlet of HX, was about 125 K, which was the main cause of turbulence appeared on streamlines and instability in the mixing of temperature appeared in the temperature contours near the outlet of HX.

Fig. 9 shows the velocity vectors of LBE, when the pump was suddenly shut down and the flow shifted from forced circulation to natural circulation without considering the wall conduction. Fig. 9 shows that the flow direction was in accordance with that of CLEAR-S and the velocity was non uniform in the different regions of the hot and cold pools during natural circulation. The velocity was comparatively high at the outlet of DHR and became low as the coolant moved upward because of the gravitational acceleration. The mass flow rate of LBE flowing through DHR in this case was 13.25 kg/s.

4.2.2. *Case-IV: NC with wall conduction*

Fig. 10 shows the temperature contours of LBE, when CLEAR-S shifted from normal operation to DHR mode. The impeller of pump

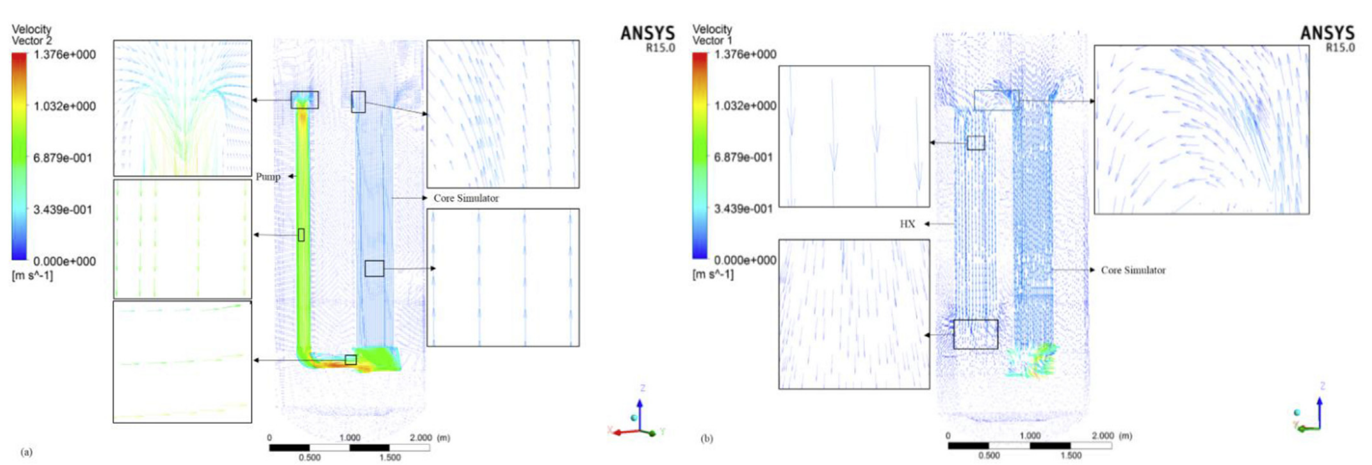

(a) The plane consist of Pump, Core simulator, CP & HP (b) The plane consist of CP, HP, Core simulator & HX

Fig. 4. The velocity vectors of LBE under forced circulation without wall conduction in CLEAR-S.

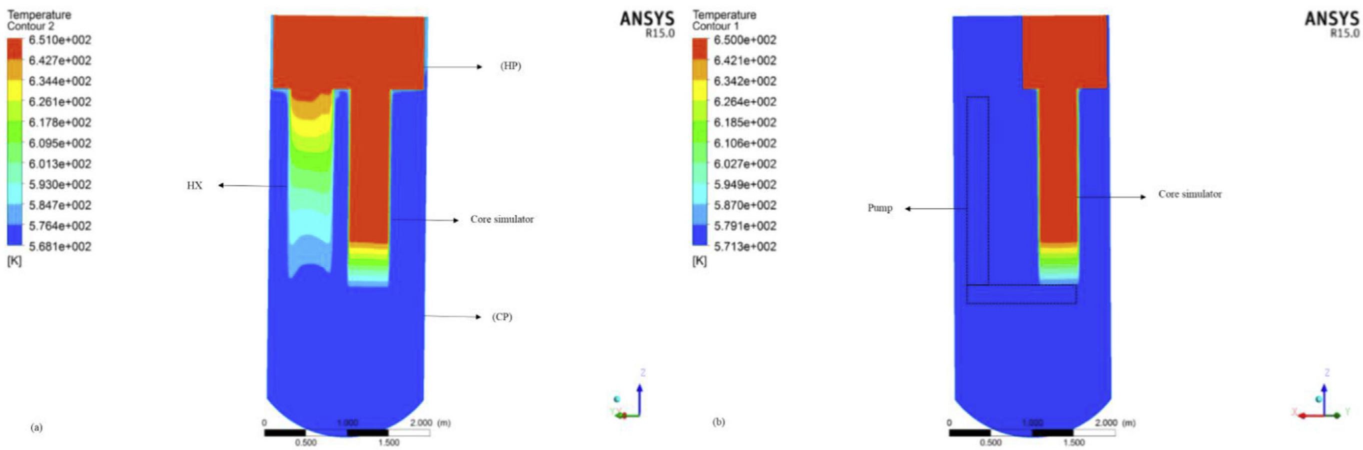

(a) The plane consist of CP, HP, Core simulator & HX (b) The plane consist of CP, HP, Core simulator & Pump

Fig. 5. The temperature contours of LBE under forced circulation conditions with wall conduction in CLEAR-S.

stopped and it provided resistance to the flow of LBE, so this flow resistance was simulated by adding porosity media model in the pump zone.

The mass flow rate increased up to 7.02 kg/s which was 0.22 kg/s higher than the mass flow rate recorded without considering wall conduction. As in natural circulation, the fluid was circulating due to the difference of fluid density in different regions and gravity. The density difference was proportional to the temperature difference, so this increase in mass flow was due to the increase of temperature difference between core simulator and HX. There was also an increase of 0.95 kg/s in the mass flow rate of DHR due to the wall conduction. This increase was because of the increase of temperature difference between DHR and the cold pool. The temperature was high in the core simulator due to the presence of electric fuel pin simulator, which heated the LBE. This hot LBE was accumulated in the hot pool and the average hot pool temperature was 640.53 K, which was 98.07 K less than that of without considering the wall conduction. The hot LBE entered the cold pool through the outlet of primary HX which was not providing any cooling during DHR mode. DHR took suction from the cold pool and removed the decay heat from the cold pool through the mixing of cold LBE and heat transfer through walls. The average cold pool temperature was 570.49 K, which was about 2.69 K higher than the average cold pool temperature calculated without wall conduction. Therefore, the decrease of temperature in the hot pool and the increase of temperature in the cold pool were because of the heat transfer through the walls of core simulator, the hot pool, HX and DHR to the cold pool. The total heat transfer through the hot pool, core simulator shell, HX shell and DHR shell was 1.6 kW, 98.1 kW, 39.2 kW and −25.05 kW, respectively. Thus, the net heat transfer through the coupled walls of all components of CLEAR-S during natural circulation was 113.85 kW, which was 65% of total heat generated by the core simulator during DHR mode. As a lot of heat transferred through the wall conduction, the temperature difference between the fluids mixed at the outlet of HX, was less than that without considering the wall conduction. Therefore, there was no turbulence or instability observed at the outlet of HX.

Fig. 11 shows the velocity vectors of LBE, when the pump was suddenly shut down and the flow shifted from forced to natural circulation. It also shows that the flow directions were in accordance with that of CLEAR-S and the velocity was not uniform in the different regions of the hot and cold pools during natural circulation. The velocity was comparatively high at the outlet of DHR. The mass flow rate of LBE flowing through DHR recorded in this case was 14.2 kg/s. There were two independent LBE circulation paths in CLEAR-S facility. In 1st path, the pump took suction of LBE from CP and LBE passed through core simulator, HP and HX before entering to CP. In 2nd path, LBE entered into DHR from CP, which delivered it back to CP after cooling. 1st path removed decay heat from the core simulator, while 2nd path removed the heat from coolant through secondary cooling.

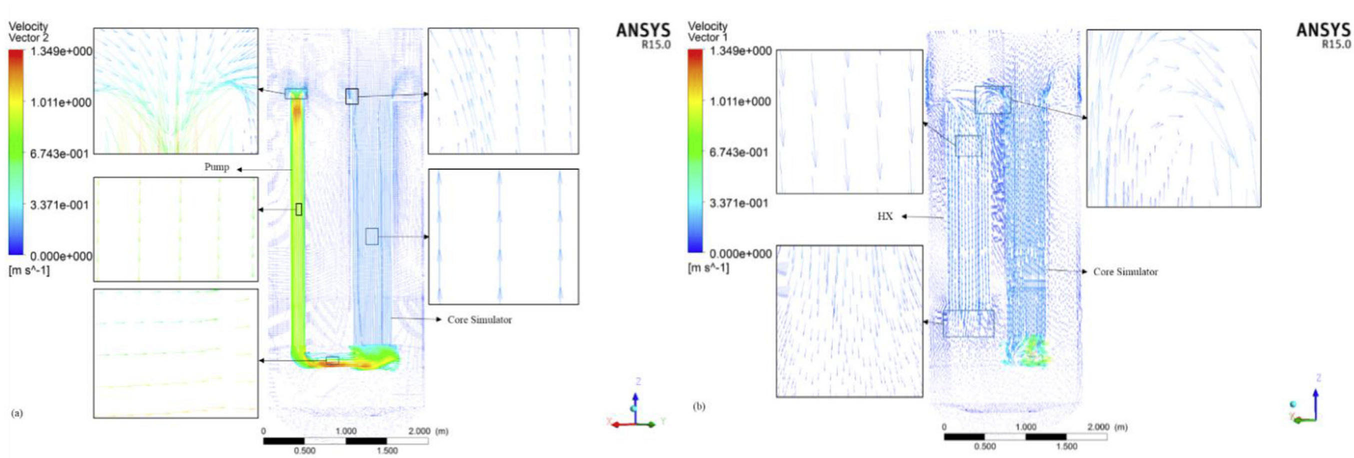

(a) The plane consist of Pump, Core simulator, CP & HP (b) The plane consist of CP, HP, Core simulator & HX

Fig. 6. The velocity vectors of LBE under forced circulation with wall conduction in CLEAR-S.

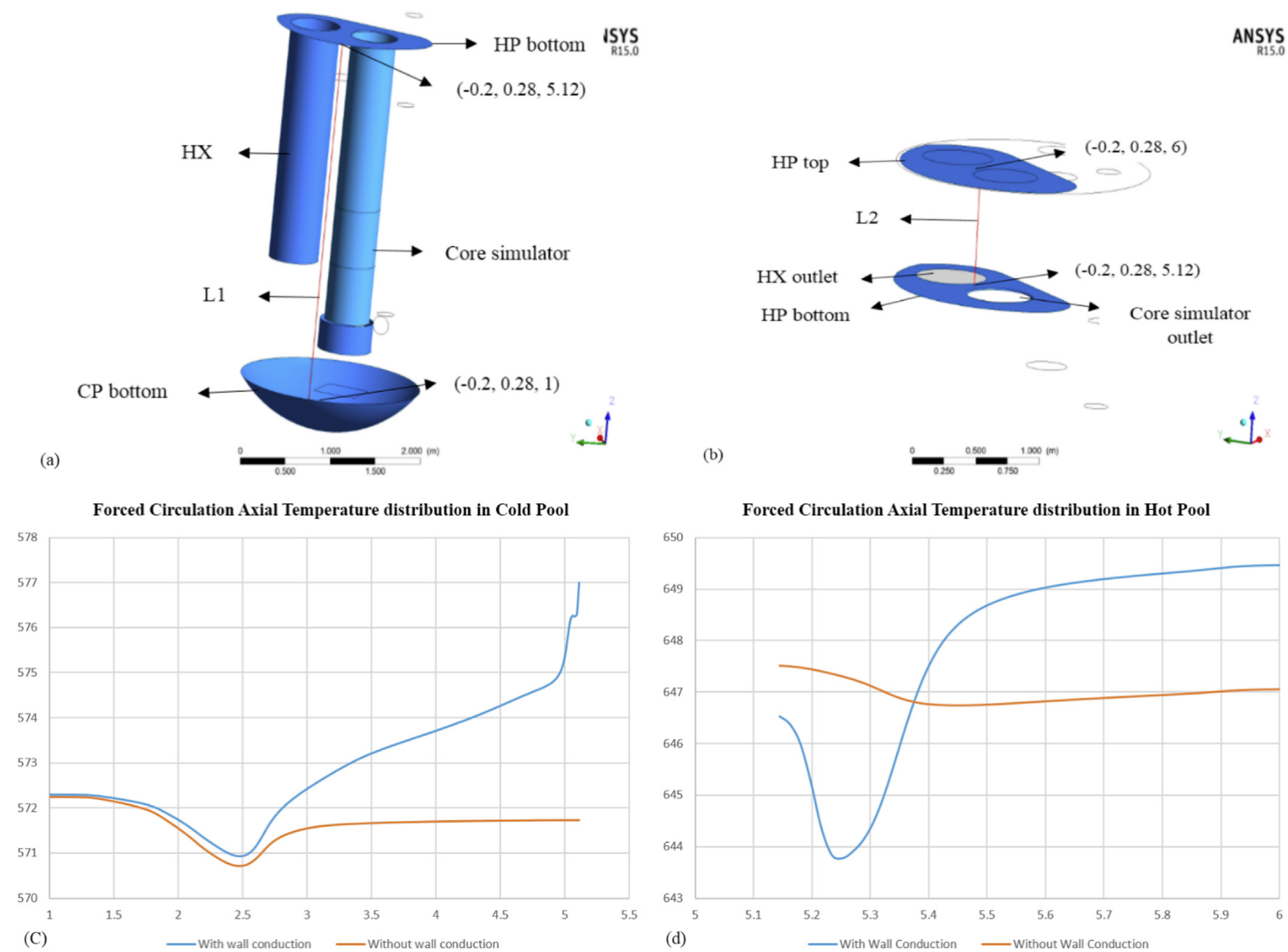

(a) The location of L1 in CP (b) The location of L2 in HP (c) The axial temperature distribution of cold pool at L1 (d) The axial temperature distribution of hot pool at L2

Fig. 7. FC with and without wall conduction in CLEAR-S.

Table 4
The temperature comparison between case I & case II.

Temperature items	FC without wall conduction (Case I)	FC with wall conduction (Case II)
T_{avg} Cold Pool	571.4 K	573.6 K
T_{max} Cold Pool	572.3 K	591.5 K
T_{min} Cold Pool	567.1 K	567.0 K
T_{avg} Hot Pool	652.0 K	648.9 K
T_{max} Hot Pool	653.5 K	650.5 K
T_{min} Hot Pool	649.0 K	627.2 K

Fig. 12 shows the axial temperature distribution with and without wall conduction in the cold and hot pools of CLEAR-S, respectively under natural circulation. The average, maximum and minimum temperatures of LBE in the cold and hot pools were tabulated in Table 5 for both cases. The difference in values between T_{max} and T_{min} was 109.2 K and 11.1 K in the cold and hot pools, respectively for case III, while this difference became 56.28 K and 16.95 K in the cold and hot pools, respectively for case IV. This high T_{max} in the cold pool of case III was near the outlet of HX where the hot LBE from the hot pool mixed with the cold pool. This big temperature difference could cause thermal stresses, which were harmful for the integrity of system. The average temperature of the hot pool in case III became 85.6 K higher than that of during normal operation, whereas on the other hand for case IV, the hot pool temperature became 8.37 K less than that during normal operation. So, wall conduction helps in removing the decay heat from the core simulator during DHR mode.

The mass flow rates of LBE through core simulator and DHR in case IV were 0.22 kg/s and 0.95 kg/s, respectively which were higher than those in case III. This small increment in the mass flow rates of core simulator and DHR were due to the temperature gradient generated by wall conduction within the cold pool.

5. Conclusions

The steady state three dimensional CFD analyses of the hot and cold pools of CLEAR-S were carried out under forced and natural circulations modes by using ANSYS FLUENT 15.0 in order to study the effects of wall conduction through the coupled walls between the cold pool and other components of CLEAR-S. Following conclusions were drawn from the above analyses.

a) The results of normal operation were in good agreement with the designed parameters of CLEAR-S, which indicated that the

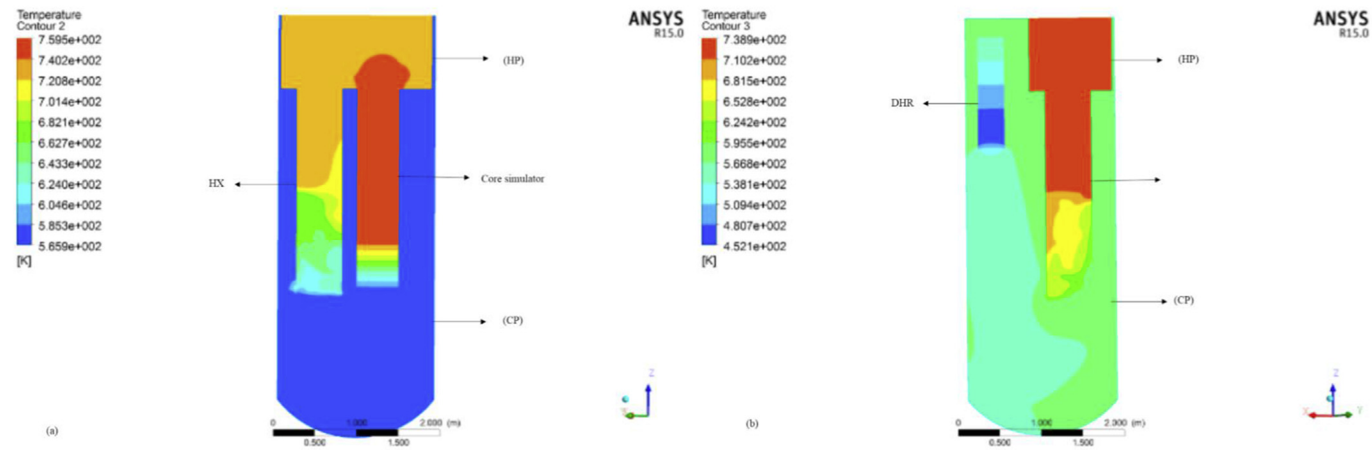

(a) The plane consist of CP, HP, Core simulator & HX (b) The plane consist of CP, HP, Core simulator & Pump

Fig. 8. The temperature contours of LBE under natural circulation conditions without wall conduction in CLEAR-S.

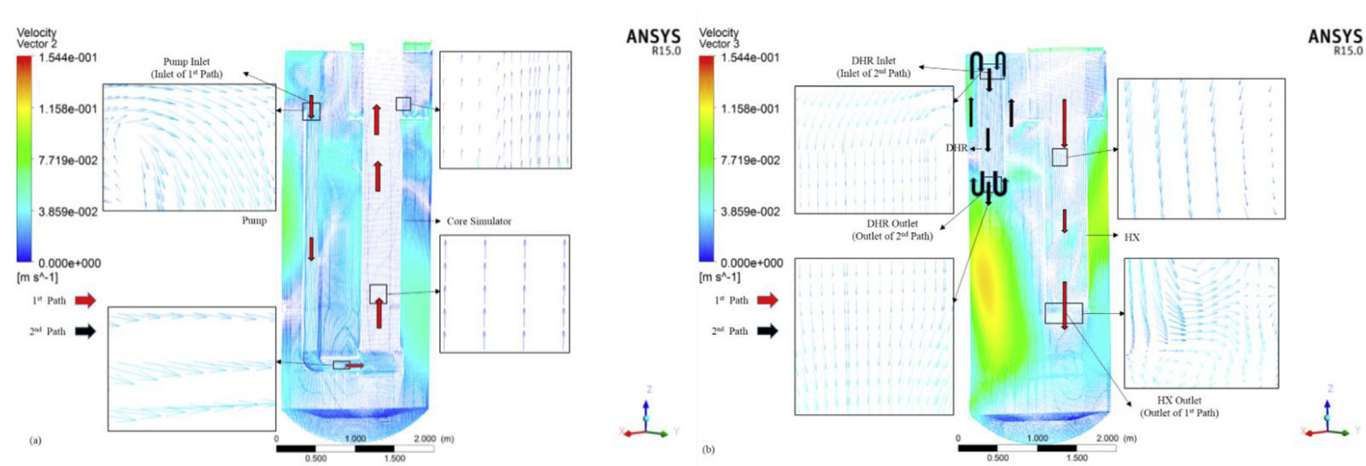

(a) The plane consist of Pump, Core simulator, CP & HP (b) The plane consist of CP, HP, DHR & HX

Fig. 9. The velocity vectors of LBE under natural circulation without wall conduction in CLEAR-S.

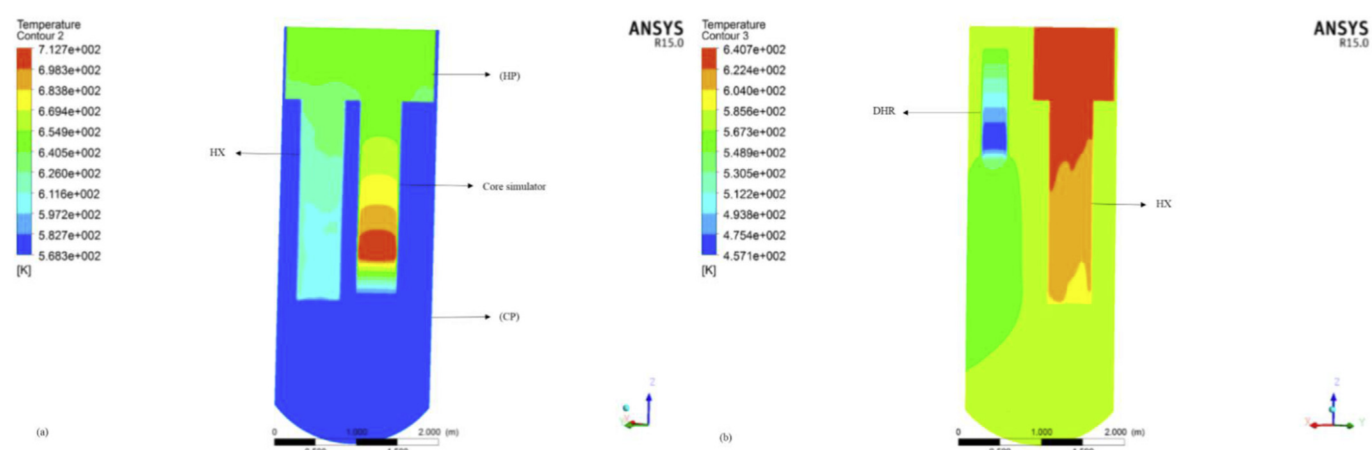

(a) The plane consist of CP, HP, Core simulator & HX (b) The plane consist of CP, HP, Core simulator & Pump

Fig. 10. The temperature contours of LBE under natural circulation conditions with wall conduction in CLEAR-S.

calculation model and the steady state simulation were correct. There was no stagnant region in the hot and cold pools of CLEAR-S during normal operation.

b) There was a decrease of 2 K in the core simulator temperature of CLEAR-S and about 3.7% of core simulator heat, was transferred through wall conduction during forced circulation.

c) There were two independent LBE circulation paths in CLEAR-S facility during natural circulation.

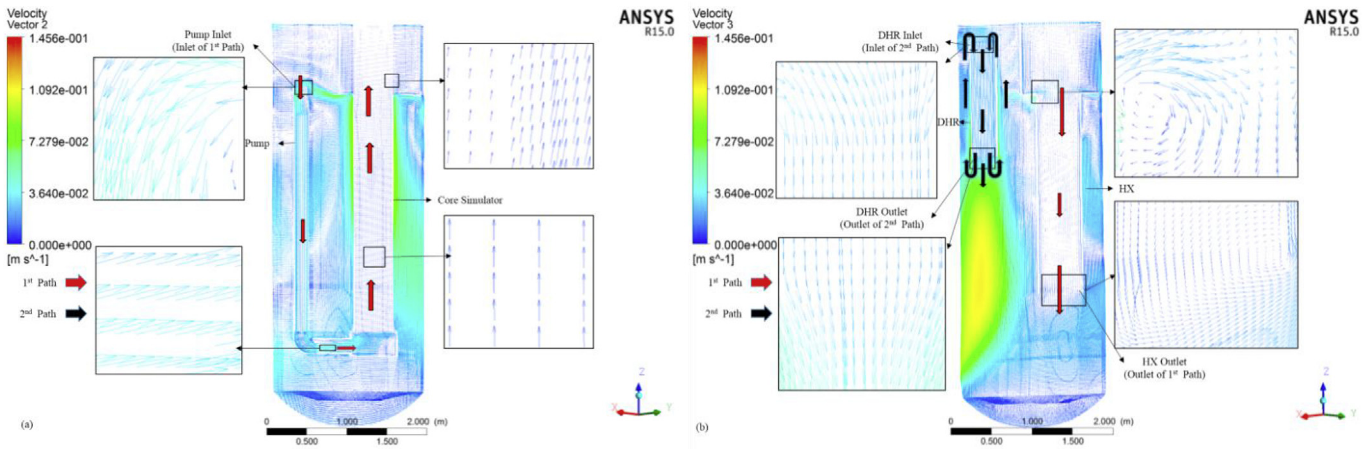

(a) The plane consist of Pump, Core simulator, CP & HP (b) The plane consist of CP, HP, DHR & HX

Fig. 11. The velocity vectors of LBE under natural circulation with wall conduction in CLEAR-S.

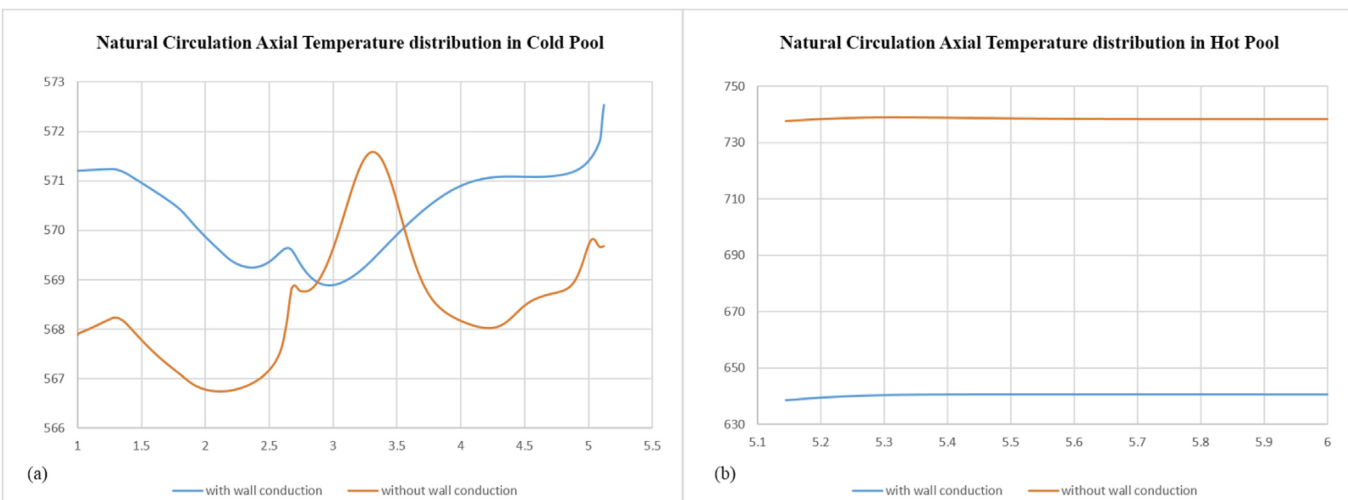

(a) The axial temperature distribution of the cold pool at L1 (b) The axial temperature distribution of the hot pool at L2

Fig. 12. NC with and without wall conduction in CLEAR-S.

Table 5
The temperature comparison between case III & case IV.

Temperature items	NC without wall conduction (Case III)	NC with wall conduction (Case IV)
T_{avg} cold pool	567.8 K	570.5 K
T_{max} cold pool	639.8 K	590.6 K
T_{min} cold pool	530.6 K	534.3 K
T_{avg} hot pool	738.6 K	640.5 K
T_{max} hot pool	748.0 K	646.2 K
T_{min} hot pool	736.9 K	629.3 K
Mass flow rate through core simulator	6.8 kg/s	7.0 kg/s
Mass flow rate through DHR	13.2 kg/s	14.2 kg/s

d) There was a decrease of 67 K in the core simulator temperatures of CLEAR-S due to the wall conduction during natural circulation, because about 65% of core simulator heat during DHR mode was transferred through coupled walls. It means that wall conduction enhanced the safety of facility by cooling the core simulator more efficiently during natural circulation. The wall conduction also added a small increment in the mass flow rate of core simulator and DHR by generating the temperature gradient within the cold pool due to the heat transfer through walls.

Acknowledgement

The author highly regards the efforts of other members in FDS Team, as well as the support from Project 2015 BAA08B01.

References

Anissimov, V., Alemberti, A., 2006. CFD Simulation of X-ADS Downcomer Thermal Stratification. https://arxiv.org/ftp/physics/papers/0601018.pdf.
ANSYS FLUENT 14.0, 2011. Theory Guied. USA.
ANSYS FLUENT 15.0, 2013. Tutorial Guide. USA.
Choi, Seok-Ki, Tae-Ho, Lee, Kim, Yeong-Il, et al., 2013. Numerical Analysis of thermal stratification in the upper plenum of MONJU fast reactor. Nucl. Eng. & Tech. 45 (2), 191–202.
Erdemir, D., Altuntop, N., 2016. Improved thermal stratification with obstacles placed inside the vertical mantled hot water tanks. Appl. Therm. Eng. 100 (5), 20–29.
Huang, Q., 2017. Status and improvement of CLAM for nuclear application. Nucl. Fusion 57 (8), 086042.
Huang, Q., Li, C., Li, Y., et al., 2007. Progress in development of China low activation martensitic steel for fusion application. J. Nucl. Mater. 367, 142–146.
Huang, Q., Baluc, N., Dai, Y., et al., 2013. Recent progress of R&D activities on reduced activation ferritic/martensitic steels. J. Nucl. Mater. 442 (1–3), S2–S8.
Jo, Byeongnam, Erkana, N., Takahashib, S., et al., 2016. Thermal stratification in a scaled-down suppression pool of the Fukushima Daiichi nuclear power plants. Nucl. Eng. Des. 305 (15), 39–50.

Kim, J.H., Roidt, R.M., Deardorff, A.F., 1993. Thermal stratification and reactor piping integrity. Nucl. Eng. Des. 139 (1), 83–95.
Liu, X., Scarpelli, N., 2015. Development of a sub-channel code for liquid metal cooled fuel assembly. Ann. Nucl. Energy 77, 425–435.
Miksch, M., Lenz, E., Löhberg, R., 1985. Loading conditions in horizontal feed water pipes of LWRs influenced by thermal shock and thermal stratification effects. Nucl. Eng. Des. 84 (2), 179–187.
Moriya, S., Tanaka, N., Katano, N., et al., 1987. Effects of Reynolds number and Richardson number on thermal stratification in hot plenum. Nucl. Eng. Des. 99, 441–451.
Nuclear Energy Agency, 2015. Handbook on Lead Bismuth Eutectic Alloy and Lead Properties, Material Compatibility, Thermal Hydraulics and Technologies.
Shibahara, M., Takata, T., Yamaguchi, A., 2013. Numerical study on thermal stratification in the upper plenum of LMFBR MONJU. Nucl. Eng. Des. 258, 226–234.
Talja, A., Hansjosten, E., 1990. Results of thermal stratification tests in a horizontal pipe line at the HDR-facility. Nucl. Eng. Des. 118 (1), 29–41.
Tarantino, M., Martelli, D., Barone, G., et al., 2015. Mixed convection and stratification phenomena in a heavy liquid metal pool. Nucl. Eng. Des. 286, 261–277.
Wu, Y., 2007. Design status and development strategy of China liquid lithium-lead blankets and related material technology. J. Nucl. Mater. 367, 1410–1415.
Wu, Y., 2008. Conceptual design of the China fusion power plant FDS-II. Fusion Eng. Des. 83 (10–12), 1683–1689.
Wu, Y., 2016a. Design and R&D progress of China lead based reactor for ADS research facility. Engineering 2 (1), 124–131.
Wu, Y., 2016b. CLEAR-S: an integrated non-nuclear test facility for China lead based research reactor. Int. J. Energy Res. 40 (14), 1951–1956.
Wu, Y., 2018. Development of high intensity D-T fusion neutron generator HINEG. Int. J. Energy Res. 42 (1), 68–72.
Wu, Y., FDS Team, 2006. Conceptual design activities of FDS series fusion power plants in China. Fusion Eng. Des. 81, 2713–2718.
Wu, Y., FDS Team, 2009. CAD-based interface programs for fusion neutron transport simulation. Fusion Eng. Des. 84 (7–11), 1987–1992.
Wu, Y., Jiang, J., Wang, M., et al., 2011. A fusion-driven subcritical system concept based on viable technologies. Nucl. Fusion 51 (10), 103036.
Wu, Y., Song, J., Zheng, H., et al., 2015. CAD-based Monte Carlo program for integrated simulation of nuclear system SuperMC. Ann. Nucl. Energy 82, 161–168.
Wu, Y., Bai, Y., Song, Y., et al., 2016a. Development strategy and conceptual design of China Lead based Research Reactor. Ann. Nucl. Energy 87, 511–516.
Wu, Y., Chen, Z., Hu, L., et al., 2016b. Identification of safety gaps for fusion demonstration reactors. Nat. Energy 1, 16154.
Cheng, Xu, Tak, Nam-il, 2006. Investigation on turbulent heat transfer to lead bismuth eutectic flows in circular tubes for nuclear applications. Nucl. Eng. Des. 236, 385–393.